

Emission and transport of cesium-137 from boreal biomass burning in the summer of 2010

Sarah A. Strode,^{1,2,3} Lesley E. Ott,¹ Steven Pawson,¹ and Theodore W. Bowyer⁴

Received 23 December 2011; revised 16 March 2012; accepted 28 March 2012; published 9 May 2012.

[1] While atmospheric concentrations of cesium-137 (^{137}Cs) have decreased since the nuclear testing era, resuspension of ^{137}Cs during biomass burning provides an ongoing emission source. The summer of 2010 was an intense biomass burning season in western Russia, with high levels of particulate matter impacting air quality and visibility. A radionuclide monitoring station in western Russia shows enhanced airborne ^{137}Cs concentrations during the wildfire period. Since ^{137}Cs binds to aerosols, satellite observations of aerosols and fire occurrences can provide a global-scale context for ^{137}Cs emissions and transport during biomass burning events. We demonstrate that high values of the Moderate Resolution Imaging Spectroradiometer aerosol optical depth coincide with detections of ^{137}Cs , and use the relationship between ^{137}Cs and aerosols to model ^{137}Cs based on organic carbon emissions and transport with the Goddard Earth Observing System, version 5 model. The model's boreal biomass burning tracer explains approximately half of the daily variability in detected ^{137}Cs concentrations at a monitoring station in western Russia. Constraining the model with the station observations, we calculate ^{137}Cs emissions of 1.5×10^{12} Bq from biomass burning north of 40° in July and August 2010. The emissions and subsequent deposition lead to a small northward redistribution of ^{137}Cs .

Citation: Strode, S. A., L. E. Ott, S. Pawson, and T. W. Bowyer (2012), Emission and transport of cesium-137 from boreal biomass burning in the summer of 2010, *J. Geophys. Res.*, 117, D09302, doi:10.1029/2011JD017382.

1. Introduction

[2] Cesium-137 (^{137}Cs) is an anthropogenic radionuclide with a half-life of 30 years. This lifetime, along with its bioavailability, makes it a concern for human health. The bulk of ^{137}Cs entered the environment from nuclear weapons testing, with the peak atmospheric fallout occurring in the 1960s [United Nations Scientific Committee on the Effects of Atomic Radiation (UNSCEAR), 2000a]. ^{137}Cs was deposited throughout the northern hemisphere, with the maximum deposition occurring in the latitudinal band around 45°N [Aoyama *et al.*, 2006]. The Chernobyl accident in 1986 introduced an additional pulse of ^{137}Cs to the environment [UNSCEAR, 2000b], especially in Europe. Although our data precede the 2011 Fukushima-Daiichi accident, this event also liberated a large amount of ^{137}Cs into the environment.

[3] Atmospheric concentrations of ^{137}Cs decreased following the nuclear-testing period, and by 2010 were very low. However, ^{137}Cs is still present in soil and vegetation, and remobilization from these reservoirs back to the atmosphere can provide a small ongoing source.

[4] Knowledge of sources of atmospheric ^{137}Cs is important to the nuclear explosion monitoring community since remote detection of ^{137}Cs and other radionuclides can be indicative of a nuclear explosion [Preparatory Commission for the Comprehensive Nuclear-Test-Ban Treaty Organization, 2011]. An International Monitoring System (IMS) for the detection of airborne radioactivity was designed and is being implemented for the Comprehensive Nuclear-Test-Ban Treaty (CTBT).

[5] Studies show increased ^{137}Cs associated with African dust events over the Canary Islands [Hernandez *et al.*, 2005; Karlsson *et al.*, 2008] and France [Menut *et al.*, 2009], and with Asian dust over Japan [Fukuyama and Fujiwara, 2008]. The ratio of ^{137}Cs to ^{90}Sr can provide information on the origin of observed dust [Igarashi *et al.*, 2001, 2005].

[6] Biomass burning provides another mechanism for the remobilization of ^{137}Cs [Paliouris *et al.*, 1995]. Amiro *et al.* [1996] determined that 40–70% of the ^{137}Cs in the fuel is released to the atmosphere during a typical field fire, and release increases with temperature. The higher levels of ^{137}Cs still present in northern ecosystems [Paliouris *et al.*, 1995] make boreal fires a particular concern for ^{137}Cs resuspension. Several studies have examined radionuclide

¹Global Modeling and Assimilation Office, NASA Goddard Space Flight Center, Greenbelt, Maryland, USA.

²Formerly at SAIC, Beltsville, Maryland, USA.

³Now at Universities Space Research Association, Columbia, Maryland, USA.

⁴Pacific Northwest National Laboratory, Richland, Washington, USA.

Corresponding author: S. A. Strode, NASA Goddard Space Flight Center, 8800 Greenbelt Rd., Code 614, Greenbelt, MD 20771, USA. (sarah.a.strode@nasa.gov)

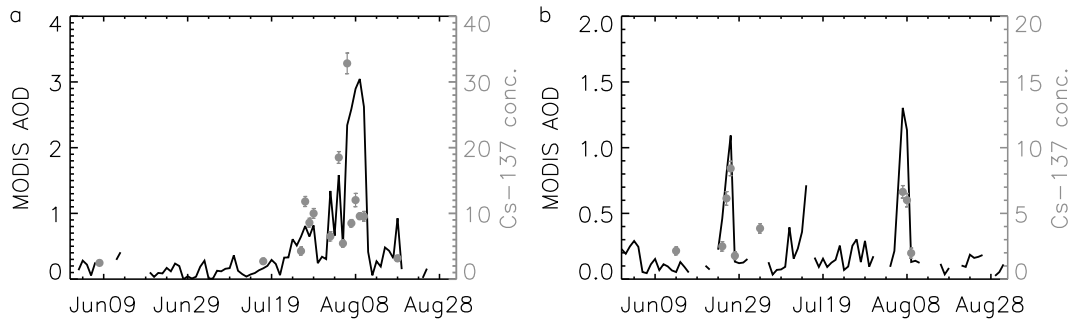


Figure 1. Comparison of MODIS AOD (black lines, left axis) at (a) Dubna and (b) Yellowknife with ^{137}Cs concentrations (gray circles, right axis) during the summer of 2010. Error bars represent the uncertainty in the ^{137}Cs measurements.

resuspension and the potential exposure of firefighters and other populations from wildfires in areas near Chernobyl [Kashparov *et al.*, 2000; Yoschenko *et al.*, 2006; Hao *et al.*, 2009]. The modeling study of Wotawa *et al.* [2006] shows that biomass burning emissions in boreal North America and Asia can explain observed summertime increases in ^{137}Cs concentrations at an IMS station located in Yellowknife, Canada in 2003 and 2004, and demonstrates the impact of intercontinental transport on atmospheric ^{137}Cs . Bourcier *et al.* [2010] examined the correlation between ^{137}Cs and levoglucosan, a product of cellulose pyrolysis used as a specific tracer of biomass burning. They found significant covariation between ^{137}Cs and levoglucosan, indicating a common source from biomass burning.

[7] The summer of 2010 was an intense biomass burning season in western Russia, with high levels of air pollutants from wildfires reaching Moscow. The fires were associated with an intense heat wave that began in June, intensified around 18 July and ended with a cold front passage on 18 August [Lau and Kim, 2012]. The heat wave was caused by atmospheric blocking [Dole *et al.*, 2011; Matsueda, 2011], and, during the period of intense fires, anticyclonic flow brought smoke into Moscow [Witte *et al.*, 2011].

[8] Fires in the Bryansk region raised concerns about whether radioactive particles could be released to the atmosphere (N. Gilbert, Russia counts environmental cost of wildfire, 2010, <http://www.nature.com/news/2010/120810/full/news.2010.404.html>). This study focuses on ^{137}Cs emissions from Russian biomass burning in July and August 2010. We compare global atmospheric model output to ground-based measurements of ^{137}Cs from IMS stations and to satellite measurements of aerosol optical depth (AOD) to constrain the boreal biomass burning source of ^{137}Cs during this intense fire season. We also examine the subsequent particulate transport and deposition of ^{137}Cs .

2. Observations of ^{137}Cs and Aerosol Optical Depth

[9] The Comprehensive Nuclear-Test-Ban Treaty Organization (CTBTO) is constructing and testing radionuclide monitoring stations as part of its International Monitoring System [Hoffmann *et al.*, 1999]. Atmospheric ^{137}Cs is expected to be in aerosol form [Yoschenko *et al.*, 2006]. IMS stations contain equipment to measure radionuclides bound to aerosols [Schulze *et al.*, 2000]. They provide daily data on

^{137}Cs and other radionuclides, through the use of high-purity germanium detectors which measure the radionuclides deposited on filters that collect aerosols from large air volume samplers. For most of the summer of 2010, ^{137}Cs concentrations were below the detection limit (typically a few $\mu\text{Bq m}^{-3}$, depending on the station) at many of the IMS stations. This study focuses on two stations located at high latitudes that detect a signal from biomass burning. These are the Yellowknife, Canada station (114.5°W, 62.4°N) previously described by Wotawa *et al.* [2006], and the Dubna site (56.7°N, 37.3°E) in the Russian Federation, which is located near the region of biomass burning in western Russia.

[10] Satellite measurements of aerosols can provide additional information related to biomass burning emissions and particulate transport of ^{137}Cs . This study used the 550 nm aerosol optical depth from the Moderate Resolution Imaging Spectroradiometer (MODIS) on the EOS Aqua satellite, which is in a sun-synchronous orbit with a 13:30 equator-crossing time. MODIS provides nearly global daily coverage [Levy *et al.*, 2009]. We obtained daily gridded data from the Giovanni online data system [Acker and Leptoukh, 2007].

[11] Figure 1 shows the relationship between MODIS AOD and ^{137}Cs at Dubna and Yellowknife during the summer of 2010. Many of the days on which ^{137}Cs is detected at Yellowknife also show enhanced AOD. In Dubna, AOD increases dramatically in late July and early August due to the intense biomass burning in the region during that period. While AOD values were typically below 0.5 in June and early July, they reach values up to three in early August. A corresponding increase is also evident in both the frequency of detection and the concentration of ^{137}Cs during the fire period, suggesting that resuspended ^{137}Cs is present in the biomass burning aerosol. Considering both sites together, the mean AOD on days when ^{137}Cs was detected is 1.2, while the mean on days without a ^{137}Cs detection is 0.18. This difference is statistically significant at the 95% level based on a Student's *t* test.

[12] The peak value of ^{137}Cs at the Dubna station, $32.83 \mu\text{Bq m}^{-3}$ on 6–7 August, is a particularly prominent feature in the time series (Figure 1a). The MODIS aerosol optical thickness and the aerosol index (AI) from the Ozone Monitoring Instrument (OMI) reached peak values over Moscow on 7 August [Witte *et al.*, 2011], and high AOD values were observed during early August at the Moscow-MSU-MU AERONET site as well [Mei *et al.*, 2011].

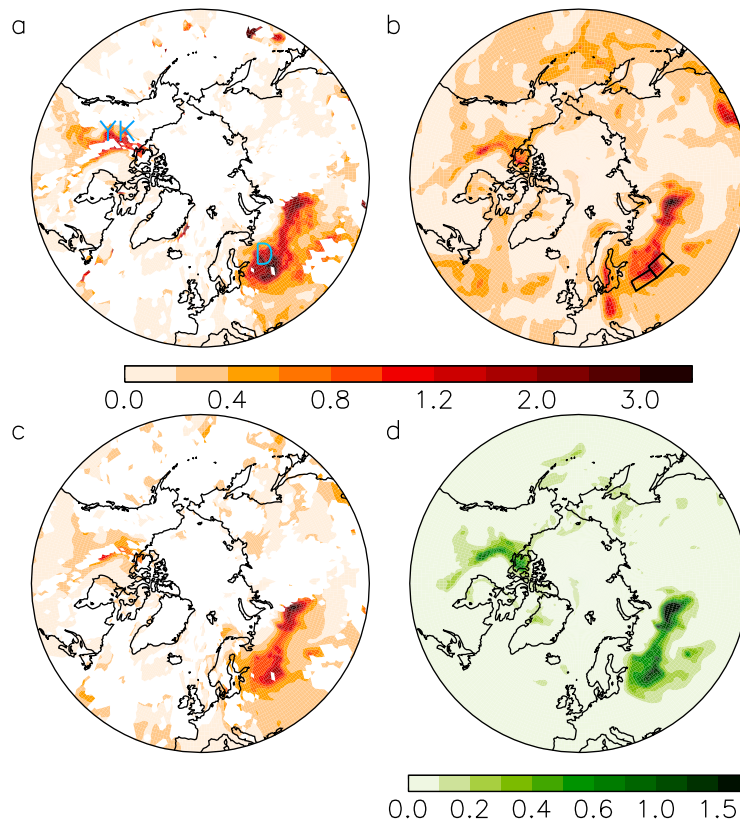


Figure 2. (a) Aerosol optical depth on 7 August 2010 from MODIS overplotted with the locations of the Dubna (D) and Yellowknife (YK) stations in blue. Areas without a valid retrieval are shown in white. (b) Model AOD overplotted with the locations of the tagged tracer regions east and west of Moscow (black boxes). (c) Model AOD shown only where valid MODIS data are present for easier comparison with Figure 2a. Areas without a valid MODIS retrieval are shown in white. (d) The boreal biomass burning POM contribution to AOD with colors corresponding to green color bar. Model results are sampled in the early afternoon in each region for consistency with the Aqua overpass.

Yurganov et al. [2011] also observed a peak in carbon monoxide (CO) on this day.

3. Model Simulation

[13] We use the Goddard Earth Observing System, version 5 (GEOS-5) global atmospheric general circulation model (AGCM) to examine the sources of the observed aerosol and ^{137}Cs concentrations, and to test the consistency of our emission estimates with the observations. The model is constrained by the Modern Era Retrospective-Analysis for Research and Applications (MERRA) meteorological fields [*Rienecker et al.*, 2011] to reproduce the winds and temperatures of the period of study. The horizontal resolution is 1.25° longitude by 1° latitude. Aerosols are simulated online within the GEOS-5 AGCM using the Goddard Chemistry, Aerosol, Radiation, and Transport (GOCART) model [*Chin et al.*, 2002; *Colarco et al.*, 2010]. The aerosol simulation includes black and organic carbon, sulfate, dust, and sea salt aerosols. We use a factor of 1.4 to convert organic carbon to particulate organic matter (POM).

[14] Biomass burning emissions of organic carbon and other aerosols come from the Global Fire Emissions Database version 3 (GFED3) [*van der Werf et al.*, 2010] with daily scaling factors [*Mu et al.*, 2011]. An initial simulation

indicated that the emissions were too low for the model to reproduce the satellite-observed AOD over western Russia during the summer of 2010. As a result, we modified daily emissions for North American, eastern and western Russian regions to reduce the model bias. The modification applied a daily varying, region-specific scaling factor to each of the three regions based on the ratio of MODIS to modeled AOD in the initial simulation over the region. The regions were chosen so that biomass burning would be the main contributor to the AOD of the region. Within each region, the scaling factor does not vary spatially, since the AOD of a single grid box is influenced by transport from surrounding areas as well as by emission into the grid box. While the resulting emissions are imperfect, they do reduce the bias in our simulation compared to the simulation with the original emissions. The improved simulation is used for the rest of this study.

[15] Figure 2 compares MODIS and modeled optical depth on 7 August, a day of strong biomass burning in western Russia. Both MODIS and the model show a strong AOD enhancement over western Russia, as well as a smaller enhancement over northern Canada. However, the model is biased low on this day and does not capture the strength of the observed enhancement in western Russia (Figures 2a and 2c). The AOD contribution from POM released by

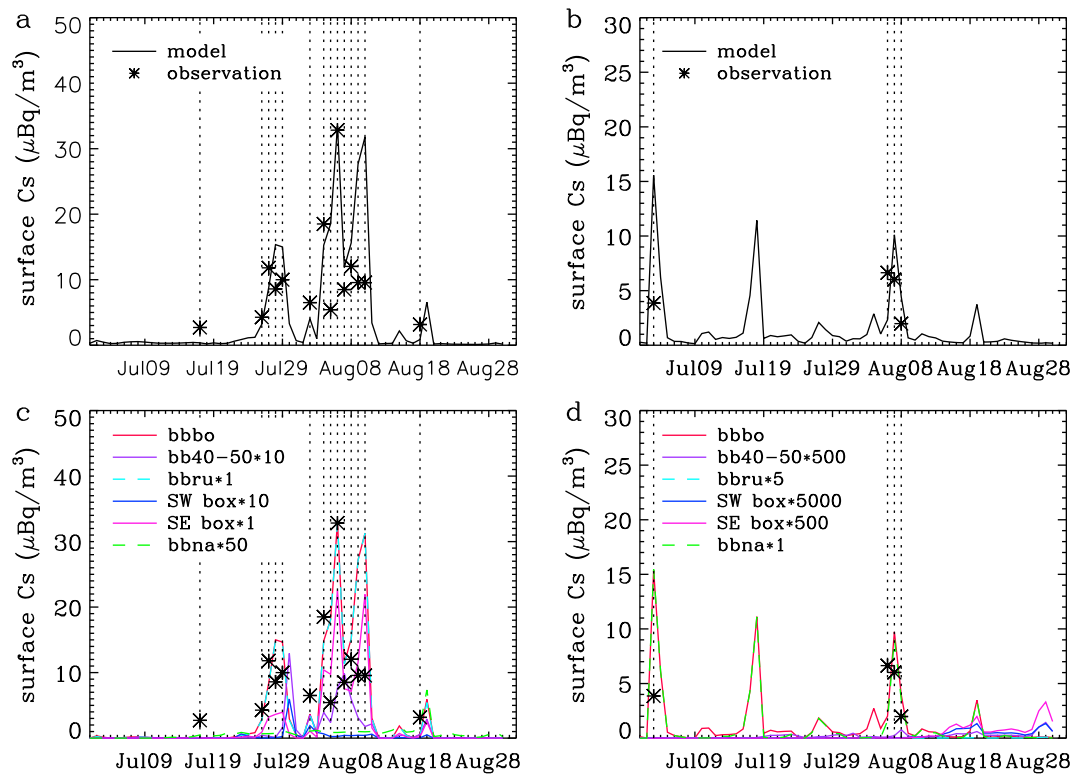


Figure 3. Observations (asterisks) and model total tracer (black line) of ^{137}Cs concentrations at (a) Dubna and (b) Yellowknife in July and August 2010. Model tagged tracers for boreal biomass burning (bbbo, red), biomass burning from 40°N to 50°N (bb30–50, purple), western Russian biomass burning (bbru, cyan), biomass burning in the southwestern (SW box, blue) and southeastern (SE box, pink) boxes, and North American biomass burning (bbna, green) are shown for (c) Dubna and (d) Yellowknife. Some tracers are scaled as described in the legend to fit on a single axis. The scaling factor is shown in the legend.

biomass burning (Figure 2d) shows the same spatial pattern as the total AOD, confirming that these enhancements are due to biomass burning.

[16] We simulate the concentration and deposition of ^{137}Cs by multiplying the modeled POM tracers by the ratio of ^{137}Cs emission to POM emission from biomass burning, since we assume that particles containing ^{137}Cs undergo the same transport and deposition processes. We neglect the radioactive decay of ^{137}Cs since the 30 year half-life is long compared with the time scale of atmospheric deposition and our period of study. Regressing the modeled POM against the Dubna ^{137}Cs data, we obtain a $^{137}\text{Cs}/\text{POM}$ ratio of 0.23 kBq kg^{-1} , and validate the resulting ^{137}Cs concentrations against the observations from Yellowknife. This method allows us to utilize the global coverage of MODIS AOD as well as the ^{137}Cs station data for model validation and to optimize our estimate of ^{137}Cs emissions.

4. Results

[17] Figure 3 compares the modeled ^{137}Cs to observations at Yellowknife and Dubna. For Dubna, we sample the model one grid box north of the station coordinates where the correlation is stronger. This may reflect uncertainty in model transport or in the fire emissions. ^{137}Cs was undetected on many days at Yellowknife, so no observations are shown on

those days. The model reproduces the timing of many of the observed peaks at both sites, suggesting that the model captures much of the impact of biomass burning on ^{137}Cs concentrations (Figures 3a and 3b). However, there are errors in the magnitude of the enhancement on individual days, which could be due to inhomogeneous ^{137}Cs distributions between different burn areas, or to errors in the strength or location of our biomass burning aerosol emissions. The true value of $^{137}\text{Cs}/\text{POM}$ is expected to vary regionally due to the variable levels of ^{137}Cs in soil and vegetation. Furthermore, since AOD is a column measurement, it does not fully constrain the surface concentration of aerosol, and model error in the vertical distribution of the biomass burning plumes could contribute to the mismatch with observed ^{137}Cs on some days.

[18] We examine the origin of the ^{137}Cs at Dubna using tagged tracers for biomass burning in different regions (Figure 3c). The tracer for western Russian BB (cyan dashed line) dominates the boreal biomass burning (red line) and total (black line) tracers at Dubna (Figures 3a and 3c). These tracers have an r^2 correlation with the detected ^{137}Cs observations of 0.49, indicating that they explain approximately half the variance in observed concentrations. Given the heterogeneity of ^{137}Cs deposits, we examine the possibility that emissions from particular regions might make greater contributions to the observed concentrations.

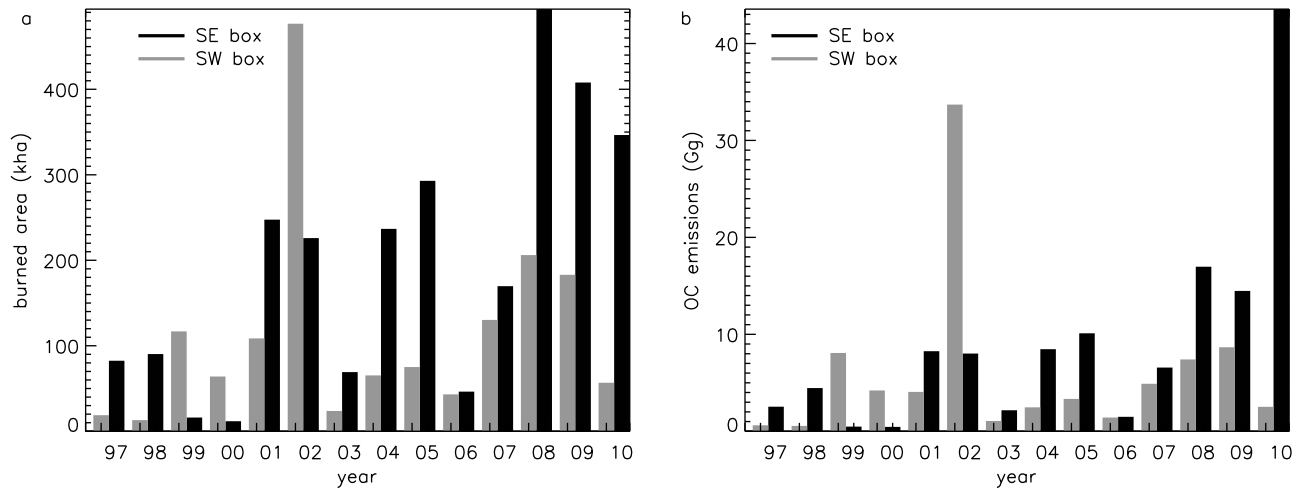


Figure 4. The 1997–2010 (a) burned area and (b) organic carbon emissions from GFED3 for the southeastern (black bars) and southwestern (gray bars) boxes. The box definitions are the same as in Figure 3.

[19] Figure 3c shows tagged tracers for the 40°N – 50°N latitude band (purple line), where zonal mean ^{137}Cs fallout was largest, for a box southwest of Moscow that includes Chernobyl (blue line), and for a box southeast of Moscow (pink line). Figure 2b shows the location of these boxes. The southeastern box has the highest correlation with the observations, $r^2 = 0.53$, while the southwest box does not correlate well with the observations. The 40°N – 50°N tracer has a weaker correlation of $r^2 = 0.34$. Since the range of ^{137}Cs concentrations is truncated by the detection limit, the data cannot be considered normally distributed. We therefore apply a nonparametric test, Spearman's rho, to determine the statistical significance of the tagged tracers. Based on this test, all of the tracers except for the southwestern box and the North American tracer have a statistically significant correlation with the Dubna observations. The southeastern box has the highest rho value, consistent with the results of the t test.

[20] Witte *et al.* [2011] used back trajectories to show that during the peak fire period southeasterly flow brought air from regions impacted by biomass burning into Moscow. Our strong correlation for the southeastern box is consistent with that result. Although the southwestern box would be expected to have more ^{137}Cs available for resuspension, it is important to note that the southwestern box tracer in Figure 3c is scaled by a factor of 10 to be visible on the plot. This shows that the contribution of the southwestern box to the POM over Dubna is much smaller than the contribution from the southeastern box. Figure 4 shows that the 2010 burned area and organic carbon emissions from the southeastern box greatly exceed those of the southwestern box, leading to the dominant contribution of the southeastern box.

[21] At Yellowknife, the total tracer is dominated by North American biomass burning (green dashed line) and shows peaks corresponding to the ^{137}Cs detections (Figures 3b and 3d). The $^{137}\text{Cs}/\text{POM}$ ratio determined for Dubna yields reasonable magnitudes for the model compared to observations at Yellowknife as well. However, the model also shows peaks at Yellowknife on days with no ^{137}Cs detection and overestimates the magnitude of the observed peak.

[22] The $^{137}\text{Cs}/\text{POM}$ ratio leads to an estimate of 1.5×10^{12} Bq ^{137}Cs emitted from biomass burning north of 40° in July and August 2010, of which 1.2×10^{12} Bq was in Eurasia and the rest in North America. For comparison, Wotawa *et al.* [2006] estimated that 4.3×10^{12} Bq and 2.2×10^{12} Bq were emitted by boreal biomass burning from May–September in 2003 and 2004, respectively. Using the monthly GFED3 burned area data set [Giglio *et al.*, 2010], we determine ^{137}Cs emissions per area burned for Canada and Russia of 2.1×10^5 and 2.6×10^5 Bq ha^{-1} , respectively. We note, however, that the ratio of organic carbon emission to burned area can vary from year to year (Figure 4), so our ratio of ^{137}Cs to burned area would also differ if a different year had been considered. None the less, our estimated values lie within the uncertainty range of 1.2×10^5 – 2.3×10^5 Bq ha^{-1} for North America and 0 – 5×10^5 Bq ha^{-1} for Siberia determined by Wotawa *et al.* [2006] for the 2003 and 2004 fires.

[23] A comparison of model deposition and emissions (Figure 5) shows the net effect of July and August boreal biomass burning on the surface distribution of ^{137}Cs . Atmospheric transport acts to spread the emissions from confined biomass burning over broader regions where it is deposited (Figures 5a and 5b). The net effect is a northward shift in deposition compared to emissions (Figure 6). Average surface concentrations of ^{137}Cs in the Northern Hemisphere midlatitudes are around 2 kBq m^{-2} [Wotawa *et al.*, 2006]. Thus, the modeled redistribution of ^{137}Cs from July and August 2010 is small compared to the existing land concentration. However, on regional scales our peak modeled ^{137}Cs deposition from boreal biomass burning (Figure 7) reaches values comparable to those measured during dust events. Fukuyama and Fujiwara [2008] measured ^{137}Cs deposition of $62.3 \text{ mBq m}^{-2} \text{ week}^{-1}$ during an Asian dust event over Japan, while the peak weekly total boreal biomass burning deposition values in this study reach hundreds of $\text{mBq m}^{-2} \text{ week}^{-1}$. Biomass burning occurs regularly in the southwestern and southeastern boxes discussed above (Figure 4). However, the 2010 emissions were anomalously high (Figure 4b). In the future, a multiyear

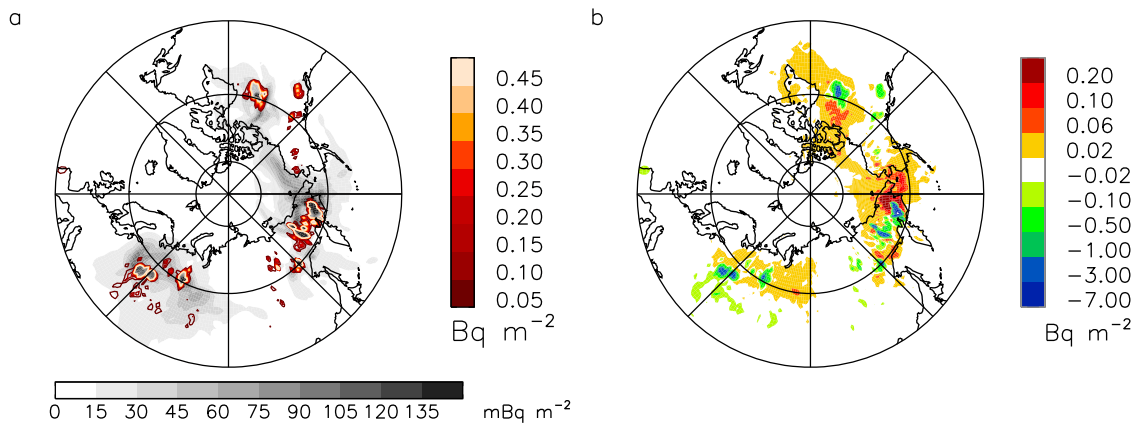


Figure 5. (a) Total boreal biomass burning emissions (red contours) for July and August 2010 overlaid on the maximum ^{137}Cs column density (gray-filled contours) at each location for the period. (b) Net surface flux of boreal biomass burning ^{137}Cs tracer, defined as deposition minus emission.

study would be useful for assessing the long-term impact of biomass burning on the ^{137}Cs distribution.

[24] The accident at the Fukushima power plant in 2011 introduced additional ^{137}Cs to the atmosphere. Although concentrations decreased by orders of magnitude with distance from accident, ^{137}Cs was detected at sites around the northern hemisphere [Hsu *et al.*, 2012]. In Europe, far downwind of the accident, observations show ^{137}Cs concentrations reaching several hundred $\mu\text{Bq/m}^3$ in Stockholm [Stohl *et al.*, 2011]. These values are much higher than the observations from the Russian fires. Deposition from the Fukushima accident has the potential to increase the resuspension of ^{137}Cs during future wildfires.

5. Conclusions

[25] Biomass burning during the summer of 2010 led to high concentrations of aerosols and other atmospheric pollutants. We find that increases in aerosol optical depth in regions affected by burning are also related to increased ^{137}Cs detections. Satellite measurements of fire activity and AOD can thus provide additional information on the emission and transport of ^{137}Cs from biomass burning. Observations of

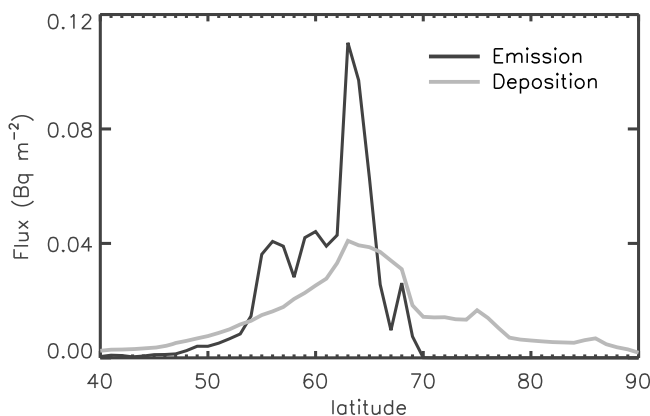


Figure 6. Latitudinal distribution of zonal mean ^{137}Cs emission (black) and deposition (gray) fluxes for the boreal biomass burning tracer in July and August 2010.

high ^{137}Cs concentrations at the Dubna station coincide with high aerosol optical depth detected by the MODIS satellite during a period of intense wildfires.

[26] We use the GEOS-5 AGCM with an embedded GOCART aerosol model to simulate aerosol concentrations during July and August 2010, and relate the modeled organic carbon to ^{137}Cs based on an emission ratio. This approach allows us to use MODIS AOD as an additional tool to validate the model simulation, providing far greater spatial coverage than would be available from ^{137}Cs concentration data alone. The model's boreal biomass burning tracer has a statistically significant correlation with detected ^{137}Cs concentrations observed at a site near the wildfires in western Russia during July and August 2010. Since ^{137}Cs has a limited number of sources to the atmosphere, it can be a useful tracer of the transport of biomass burning emissions.

[27] Constraining the model with ^{137}Cs observations yields a best guess estimate of $0.23 \text{ kBq } ^{137}\text{Cs kg}^{-1} \text{ POM}$, leading to total boreal biomass burning ^{137}Cs emissions of $1.5 \times 10^{12} \text{ Bq}$ for July and August 2010. This corresponds

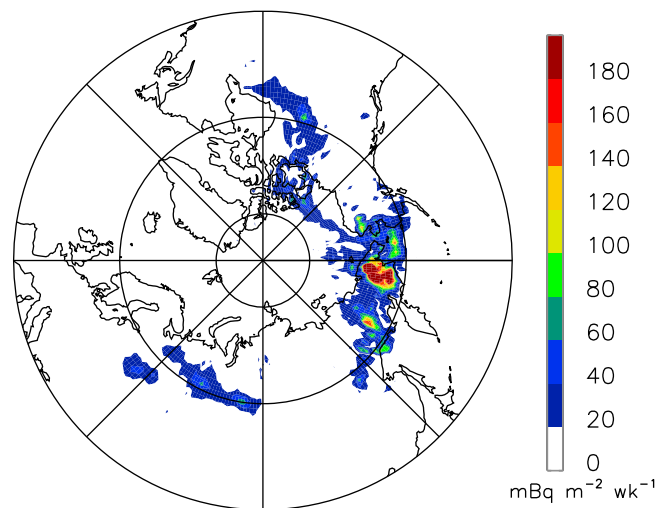


Figure 7. Maximum modeled weekly ^{137}Cs deposition value reached in July–August at each location.

to emissions of 2.1×10^5 and 2.6×10^5 Bq ha⁻¹ for Canada and Russia, respectively, consistent with the 2×10^5 Bq ha⁻¹ estimate of *Wotawa et al.* [2006].

[28] Satellite-based information on AOD, ground-based measurements of radioactivity, and other information could be combined with atmospheric transport modeling to better constrain ¹³⁷Cs emission sources. The correlation between observed measurements using AOD and the ground-based IMS radionuclide sensors imply that resuspended ¹³⁷Cs can be strongly tied to phenomena such as wildfires. The net effect of the biomass burning emissions and subsequent deposition in our period of study is a small northward redistribution of ¹³⁷Cs. Boreal forest fires are a recurring phenomenon, and the methods described in this paper could be extended to help predict large-scale impacts of future fire scenarios on the ¹³⁷Cs distribution.

[29] **Acknowledgments.** We are grateful to NASA for funding this work through the Modeling, Analysis and Prediction program and for providing high-performance computing resources on “Discover” at the NCCS. The Giovanni online data system is maintained by the NASA GES DISC. We thank Arlindo da Silva and Anton Darnenov for helpful discussions.

References

- Acker, J. G., and G. Leptoukh (2007), Online analysis enhances use of NASA Earth science data, *Eos Trans. AGU*, 88(2), 14, doi:10.1029/2007EO020003.
- Amiro, B. D., S. C. Sheppard, F. L. Johnston, W. G. Evenden, and D. R. Harris (1996), Burning radionuclide question: What happens to iodine, cesium and chlorine in biomass fires?, *Sci. Total Environ.*, 187, 93–103, doi:10.1016/0048-9697(96)05125-X.
- Aoyama, M., K. Hirose, and Y. Igarashi (2006), Re-construction and updating our understanding on the global weapons tests ¹³⁷Cs fallout, *J. Environ. Monit.*, 8, 431–438, doi:10.1039/b512601k.
- Bourcier, L., K. Sellegri, O. Masson, R. Zangrando, C. Barbante, A. Gambaro, J.-M. Pichon, J. Boulon, and P. Laj (2010), Experimental evidence of biomass burning as a source of atmospheric ¹³⁷Cs, puy de Dôme (1465 m a.s.l.), France, *Atmos. Environ.*, 44, 2280–2286, doi:10.1016/j.atmosenv.2010.04.017.
- Chin, M., P. Ginoux, S. Kinne, O. Torres, B. N. Holben, B. N. Duncan, R. V. Martin, J. A. Logan, A. Higurashi, and T. Nakajima (2002), Tropospheric aerosol optical thickness from the GOCART model and comparisons with satellite and sun photometer measurements, *J. Atmos. Sci.*, 59, 461–483, doi:10.1175/1520-0469(2002)059<0461:TAOTFT>2.0.CO;2.
- Colarco, P., A. da Silva, M. Chin, and T. Diehl (2010), Online simulations of global aerosol distributions in the NASA GEOS-4 model and comparisons to satellite and ground-based aerosol optical depth, *J. Geophys. Res.*, 115, D14207, doi:10.1029/2009JD012820.
- Dole, R., M. Hoerling, J. Perlwitz, J. Eischeid, P. Pegion, T. Zhang, X.-W. Quan, T. Xu, and D. Murray (2011), Was there a basis for anticipating the 2010 Russian heat wave?, *Geophys. Res. Lett.*, 38, L06702, doi:10.1029/2010GL046582.
- Fukuyama, T., and H. Fujiwara (2008), Contribution of Asian dust to atmospheric deposition of radioactive cesium (¹³⁷Cs), *Sci. Total Environ.*, 405, 389–395, doi:10.1016/j.scitotenv.2008.06.037.
- Giglio, L., J. T. Randerson, G. R. van der Werf, P. S. Kasibhatla, G. J. Collatz, D. C. Morton, and R. S. DeFries (2010), Assessing variability and long-term trends in burned area by merging multiple satellite fire products, *Biogeosciences*, 7(3), 1171–1186, doi:10.5194/bg-7-1171-2010.
- Hao, W. M., O. O. Bondarenko, S. Zibitsev, and D. Hutton (2009), Vegetation fires, smoke emissions, and dispersion of radionuclides in the Chernobyl exclusion zone, in *Wildland Fires and Air Pollution*, *Dev. Environ. Sci.*, vol. 8, edited by A. Bytnerowicz et al., chap. 12, pp. 265–276, Elsevier, Amsterdam.
- Hernández, F., S. Alonso-Pérez, J. Hernández-Armas, E. Cuevas, L. Karlsson, and P. M. Romero-Campos (2005), Influence of major African dust intrusions on the ¹³⁷Cs and ⁴⁰K activities in the lower atmosphere at the island of Tenerife, *Atmos. Environ.*, 39, 4111–4118, doi:10.1016/j.atmosenv.2005.03.032.
- Hoffmann, W., R. Kebeasy, and P. Firbas (1999), Introduction to the verification regime of the Comprehensive Nuclear-Test-Ban Treaty, *Phys. Earth Planet. Inter.*, 113, 5–9, doi:10.1016/S0031-9201(99)00027-8.
- Hsu, S.-C., C.-A. Huh, C.-Y. Chan, S.-H. Lin, F.-J. Lin, and S. C. Liu (2012), Hemispheric dispersion of radioactive plume laced with fission nuclides from the Fukushima nuclear event, *Geophys. Res. Lett.*, 39, L00G22, doi:10.1029/2011GL049986.
- Igarashi, Y., M. Aoyama, K. Hirose, T. Miyao, and S. Yabuki (2001), Is it possible to use ⁹⁰Sr and ¹³⁷Cs as tracers for the Aeolian dust transport?, *Water Air Soil Pollut.*, 130, 349–354.
- Igarashi, Y., M. Aoyama, K. Hirose, P. Povinec, and S. Yabuki (2005), What anthropogenic radionuclides (⁹⁰Sr and ¹³⁷Cs) in atmospheric deposition, surface soils and Aeolian dusts suggest for dust transport over Japan, *Water Air Soil Pollut.: Focus*, 5, 51–69, doi:10.1007/s11267-005-0726-z.
- Karlsson, L., F. Hernandez, S. Rodríguez, M. López-Pérez, J. Hernandez-Armas, S. Alonso-Pérez, and E. Cuevas (2008), Using ¹³⁷Cs and ⁴⁰K to identify natural Saharan dust contributions to PM10 concentrations and air quality impairment in the Canary Islands, *Atmos. Environ.*, 42, 7034–7042, doi:10.1016/j.atmosenv.2008.06.016.
- Kashparov, V. A., S. M. Lundin, A. M. Kadygrib, V. P. Protsak, S. E. Levitchuk, V. I. Yoschenko, V. A. Kashpur, and N. M. Talerko (2000), Forest fires in the territory contaminated as a result of the Chernobyl accident: Radioactive aerosol resuspension and exposure of fire-fighters, *J. Environ. Radioact.*, 51, 281–298, doi:10.1016/S0265-931X(00)00082-5.
- Lau, W. K. M., and K.-M. Kim (2012), The 2010 Pakistan flood and Russian heat wave: Teleconnection of hydrometeorological extremes, *J. Hydrometeorol.*, 13, 392–403, doi:10.1175/JHM-D-11-016.1.
- Levy, R. C., L. A. Remer, D. Tanré, S. Mattoo, and Y. J. Kaufman (2009), Algorithm for remote sensing of tropospheric aerosol over dark targets from MODIS: Collections 005 and 051: Revision 2, report, 96 pp., NASA Goddard Space Flight Cent., Greenbelt, Md. [Available at http://modis-atmos.gsfc.nasa.gov/MOD04_L2/atbd.html.]
- Matsueda, M. (2011), Predictability of Euro-Russian blocking in summer of 2010, *Geophys. Res. Lett.*, 38, L06801, doi:10.1029/2010GL046557.
- Mei, L., et al. (2011), Integration of remote sensing data and surface observations to estimate the impact of the Russian wildfires over Europe and Asia during August 2010, *Biogeosciences*, 8, 3771–3791, doi:10.5194/bg-8-3771-2011.
- Menut, L., O. Masson, and B. Bessagnet (2009), Contribution of Saharan dust on radionuclide aerosol activity levels in Europe? The 21–22 February 2004 case study, *J. Geophys. Res.*, 14, D16202, doi:10.1029/2009JD011767.
- Mu, M., et al. (2011), Daily and 3-hourly variability in global fire emissions and consequences for atmospheric model predictions of carbon monoxide, *J. Geophys. Res.*, 116, D24303, doi:10.1029/2011JD016245.
- Paliouris, G., H. W. Taylor, R. W. Wein, J. Svoboda, and B. Mierzynski (1995), Fire as an agent in redistributing fallout ¹³⁷Cs in the Canadian boreal forest, *Sci. Total Environ.*, 160–161, 153–166, doi:10.1016/0048-9697(95)04353-3.
- Preparatory Commission for the Comprehensive Nuclear-Test-Ban Treaty Organization (2011), The CTBT verification regime: Monitoring the Earth for nuclear explosions, report, Vienna. [Available at http://www.ctbto.org/fileadmin/user_upload/public_information/2011/2011_Verification_Regime_web.pdf.]
- Rienecker, M. M., et al. (2011), MERRA: NASA’s Modern-Era Retrospective Analysis for Research and Applications, *J. Clim.*, 24, 3624–3648, doi:10.1175/JCLI-D-11-00015.1.
- Schulze, J., M. Auer, and R. Werzi (2000), Low level radioactivity measurement in support of the CTBTO, *Appl. Radiat. Isot.*, 53, 23–30, doi:10.1016/S0969-8043(00)00182-2.
- Stohl, A., P. Seibert, G. Wotawa, D. Arnold, J. F. Burkhart, S. Eckhardt, C. Tapia, A. Vargas, and T. J. Yasunari (2011), Xenon-133 and caesium-137 releases into the atmosphere from the Fukushima Dai-ichi nuclear power plant: Determination of the source term, atmospheric dispersion, and deposition, *Atmos. Chem. Phys. Discuss.*, 11, 28,319–28,394, doi:10.5194/acpd-11-28319-2011.
- United Nations Scientific Committee on the Effects of Atomic Radiation (UNSCEAR) (2000a), Annex C: Exposures to the public from man-made sources of radiation, in *Sources and Effects of Ionizing Radiation*, vol. 1, *Sources*, UNSCEAR 2000 report, pp. 157–291, Vienna.
- United Nations Scientific Committee on the Effects of Atomic Radiation (UNSCEAR) (2000b), Annex J: Exposures and effects of the Chernobyl accident, in *Sources and Effects of Ionizing Radiation*, vol. 2, *Effects*, UNSCEAR 2000 report, pp. 451–566, Vienna.
- van der Werf, G. R., J. T. Randerson, L. Giglio, G. J. Collatz, M. Mu, P. S. Kasibhatla, D. C. Morton, R. S. DeFries, Y. Jin, and T. T. van Leeuwen (2010), Global fire emissions and the contribution of deforestation, savanna, forest, agricultural, and peat fires (1997–2009), *Atmos. Chem. Phys.*, 10, 11,707–11,735, doi:10.5194/acp-10-11707-2010.
- Witte, J. C., A. R. Douglass, A. da Silva, O. Torres, R. Levy, and B. N. Duncan (2011), NASA A-Train and Terra observations of the

- 2010 Russian wildfires, *Atmos. Chem. Phys.*, *11*, 9287–9301, doi:10.5194/acp-11-9287-2011.
- Wotawa, G., L.-E. De Geer, A. Becker, R. D'Amours, M. Jean, R. Servranckx, and K. Ungar (2006), Inter- and intra-continental transport of radioactive cesium released by boreal forest fires, *Geophys. Res. Lett.*, *33*, L12806, doi:10.1029/2006GL026206.
- Yoschenko, V. I., et al. (2006), Resuspension and redistribution of radionuclides during grassland and forest fires in the Chernobyl exclusion zone: part I. Fire experiments, *J. Environ. Radioact.*, *86*, 143–163, doi:10.1016/j.jenvrad.2005.08.003.
- Yurganov, L. N., et al. (2011), Satellite- and ground-based CO total column observations over 2010 Russian fires: Accuracy of top-down estimates based on thermal IR satellite data, *Atmos. Chem. Phys.*, *11*, 7925–7942, doi:10.5194/acp-11-7925-2011.